JGR Oceans

RESEARCH ARTICLE
10.1029/2022JC019518

The Role of Deep Winter Mixing and Wind-Driven Surface Ekman Transport in Supplying Oceanic Nitrate to a Temperate Shelf Sea

Xiaoyan Wei[1], Joanne Hopkins[1], Marilena Oltmanns[2], Clare Johnson[3], and Mark Inall[3]

[1]National Oceanography Centre, Liverpool, UK, [2]National Oceanography Centre, Southampton, UK, [3]Scottish Association for Marine Science, Oban, UK

Key Points:

- Interannual variations in deep winter mixing and pre-bloom surface nitrate levels along the North West (NW) European shelf edge vary with latitude
- Winter winds drive a mean surface nitrate transport of 3.7–5.4 mmol m^{-1} s^{-1} off-shelf south of 50°N and >6.6 mmol m^{-1} s^{-1} on-shelf further north
- Year-to-year variations in the winter oceanic nitrate supply to shelf seas depends on deep winter mixing and regional wind direction/speed

Supporting Information:

Supporting Information may be found in the online version of this article.

Correspondence to:

X. Wei,
xwei@noc.ac.uk

Citation:

Wei, X., Hopkins, J., Oltmanns, M., Johnson, C., & Inall, M. (2024). The role of deep winter mixing and wind-driven surface Ekman transport in supplying oceanic nitrate to a temperate shelf sea. *Journal of Geophysical Research: Oceans*, *129*, e2022JC019518. https://doi.org/10.1029/2022JC019518

Received 30 NOV 2022
Accepted 5 DEC 2023

Author Contributions:

Conceptualization: Xiaoyan Wei, Joanne Hopkins
Data curation: Joanne Hopkins
Formal analysis: Xiaoyan Wei, Joanne Hopkins, Marilena Oltmanns
Investigation: Xiaoyan Wei, Marilena Oltmanns
Methodology: Xiaoyan Wei, Joanne Hopkins, Marilena Oltmanns, Clare Johnson, Mark Inall
Software: Xiaoyan Wei, Mark Inall
Validation: Xiaoyan Wei

Abstract

Nutrient availability across temperate continental shelves just before the onset of seasonal stratification is an important control on the spring phytoplankton bloom. However, shelf-scale quantification of nitrate supply from the open ocean during winter, a major source of shelf nitrate, is lacking. We used an objective analysis of subsurface ocean temperature (2000–2021), a nitrate climatology and an atmosphere reanalysis to quantify: (a) the interannual variability of the winter surface mixed layer depth (MLD) along the North West (NW) European shelf break, (b) oceanic surface nitrate concentration following deep winter mixing (i.e., nitrate recharge), and (c) the pre-bloom wind-driven cross-shelf surface Ekman transport. Our results show clear latitude-dependent regimes. In the north, across the Rockall-Malin and Hebrides shelves, winter winds drive an average on-shelf surface nitrate transport of 6.9 and 13.1 mmol m^{-1} s^{-1}, respectively. In the south, adjacent to the Celtic and Armorican shelves, large year-to-year variability in the MLD across strong subsurface vertical nitrate gradients results in significant year-to-year variability (up to ~6 mmol m^{-3}) in the winter nitrate recharge. However, the winter surface Ekman transport is off-shelf with an average magnitude of 3.7 and 5.4 mmol m^{-1} s^{-1} across the Armorican and Celtic Sea shelves, respectively. Our study provides the first shelf-scale estimates of interannual variability in the winter wind-driven surface nitrate supply to the NW European Shelf. The limitations of this study imposed by reliance on a nitrate climatology highlights the need for sustained biogeochemical sampling across the shelf slope to better understand cross-shelf nitrate transport processes.

Plain Language Summary

The nutrients present in mid-latitude shelves play a crucial role in influencing the growth of spring phytoplankton, particularly before warm layers form over cold ones. Despite this importance, we lack knowledge about how much nitrate moves from the ocean to these shelves during winter. To address this, we investigated the movement of nitrate near the North West (NW) European shelf break caused by deep winter mixing and surface winds between 2000 and 2021. Our findings reveal latitude-based differences in these processes. In northern regions, powerful winter winds along the shelf break transport a significant amount of nitrate to shelves like Rockall-Malin and Hebrides, with notable yearly variations. In contrast, southern areas such as Celtic and Armorican shelves see nitrate being carried from shelves to the ocean due to winter winds. These shelves also witness varying nitrate levels in winter due to shifts in mixed surface layer depth and abrupt vertical nitrate changes. While our study provides initial estimates of year-to-year nitrate variations on the NW European Shelf due to winter winds, our conclusions rely on nitrate climatology. A deeper comprehension of nitrate movement across the shelf break before spring bloom necessitates extended observations both on and off the shelves.

1. Introduction

The coastal ocean plays a critical role in the global carbon cycle and marine ecosystem. Coastal and shelf seas support 10%–30% of the total marine primary productivity (Behrenfeld et al., 2005; Field et al., 1998), underpinning the base of a productive shelf sea ecosystem that provides over 90% of commercial fish catches (Pauly et al., 2002). Globally, about 56%–58% and 85%–90% of the phosphorus and nitrogen required respectively by shelf seas to maintain their high productivity are supplied from the ocean (Liu et al., 2010). The coastal and shelf seas are also a net sink of atmospheric carbon dioxide (Laruelle et al., 2010), notably across temperate northern hemisphere shelves (Roobaert et al., 2019), where the uptake of CO_2, driven by both biological growth and CO_2

Visualization: Xiaoyan Wei, Joanne Hopkins, Clare Johnson
Writing – original draft: Xiaoyan Wei, Joanne Hopkins
Writing – review & editing: Xiaoyan Wei, Joanne Hopkins, Marilena Oltmanns, Clare Johnson, Mark Inall

solubility, and the ultimate export of carbon off-shelf is commonly referred to as the shelf sea carbon pump (Kitidis et al., 2019; Thomas et al., 2004; Tsunogai et al., 1999).

Biological and physical processes together maintain the shelf sea carbon pump, particularly across shelves where the average circulation patterns are slow and the exchange times with the open ocean are greater than a seasonal cycle. However, the magnitude and timing of physical processes that supply new, oceanic origin nutrients to the shelf remain unclear. Recent observations of interannual differences in the carbon and nutrient pools across both the North Sea and Celtic Sea, the widest sectors of the temperate North West (NW) European shelves, have highlighted the importance of year-to-year variability in ocean-shelf exchange and the impact that large exchange events are likely to play in maintaining the continental shelf carbon pump (Chaichana et al., 2019; Humphreys et al., 2019; Sharples et al., 2019). Cross-shelf exchange events can both export water rich in dissolved organic carbon, that has accumulated over the past growing seasons, to the deep ocean, and supply new oceanic origin water rich in inorganic macronutrients that is required to replenish depleting nutrient pools onto the shelf.

The NW European shelves are typically considered to be resource (nutrient and light) driven systems, where the annual capacity for new primary production and the magnitude of the spring phytoplankton bloom are set, to first order, by the pre-bloom concentration of macronutrients (Heath & Beare, 2008; Mathis et al., 2019). In the northern North Sea, a sufficient number of high-quality in-situ nutrient measurements have been made to construct time series that reveal interannual to decadal variability in winter (December-February) nitrate concentrations of ∼1–2 mmol m^{-3}. This variability is thought to be associated with wind-driven shifts in the location of strong horizontal gradients in mean winter nutrient concentrations to the northwest of Shetland (Pätsch et al., 2020). Across other sectors of the NW European shelf, however, data coverage is spatially and temporally patchy, and long-term time series of nutrient concentrations are rare, prohibiting robust analysis of interannual variability. At a limited number of locations where reliable comparisons between selected years can be made, variability of at least 1 mmol m^{-3} is observed. For example, between 2014 and 2015 the pre-bloom (March) nitrate concentration in the central Celtic Sea decreased from 8 to 7 mmol m^{-3} (Humphreys et al., 2019; Ruiz-Castillo et al., 2019).

The surface nutrient concentration of North East Atlantic water depends on the depth of winter mixing (Hartman et al., 2010, 2014; Oschlies, 2002). In the upper waters of Rockall Trough, interannual variability of nitrate concentrations is also known to be linked to the Subpolar Gyre and the relative proportions of subtropical versus subpolar origin water entering the trough (Johnson et al., 2013). Projected decreases in the NW European shelf primary production in future climate scenarios are linked to winter mixed layer shoaling and subsequent reduced oceanic nutrient supplies to the shelf (Gröger et al., 2013; Holt et al., 2012; Mathis & Mikolajewicz, 2020; Mathis et al., 2019). Likewise, some of the observed year-to-year differences in pre-bloom nitrate concentration in the Celtic Sea can also be explained by the present-day variability in the depth of oceanic winter mixing at the shelf break (Ruiz-Castillo et al., 2019).

Multiple seasonally and spatially variable ocean-shelf exchange processes are at play along the NW European shelf edge (Huthnance et al., 2022). The prevailing winds and passage of weather patterns are usually considered as a leading order driver of exchange and transport. Short-term variability (seasonal-interannual) of inflow into the North Sea is linked to the wind conditions (Mathis et al., 2015; Sheehan et al., 2017), especially during the winter, and can communicate changes in North East Atlantic ocean properties to the shelf (Koul et al., 2019). On the Malin Shelf, intense winter storms drive on-shelf transport of oceanic origin water toward the coast (Jones et al., 2020). In a large-scale and decade-averaged sense, the NW European shelf has an overall downwelling circulation: water is brought on-shelf within the surface Ekman layer and is exported within the bottom Ekman layer, associated with the prevailing wind stress and poleward slope currents, respectively (Holt et al., 2009; Huthnance et al., 2022). Modeling studies reveal that, for the length of the shelf break, between 48°N and 61°N, this downwelling circulation can drive a mean on-shelf nitrate flux of 4 mmol m^{-1} s^{-1} above 150 m between December and March (Holt et al., 2012). The exception is over the southern sectors (i.e., Celtic Sea, Armorican shelf) where prevailing south-westerly winds can drive an upwelling regime: off-shelf at the surface, and on-shelf at depth (Pingree et al., 1984, 1986). However, the surface and bottom Ekman transport components do not balance each other within each of the sectors due to nonhomogeneous water properties along the shelf and non-Ekman flows around the shelf edge (Holt et al., 2009). There is large uncertainty around the dominant export processes in the bottom layer (Huthnance et al., 2022).

The important role of wind in driving large-scale circulation and significant exchange and transport has been widely acknowledged (Holt et al., 2012; Huthnance et al., 2022). Therefore, in this paper we focus on the

wind-driven interannual variability in cross-shelf exchange and near-surface transport of oceanic nitrate onto the temperate NW European shelf seas. We draw upon the EN4 objective analysis time series of subsurface temperature profiles, the World Ocean Atlas (WOA) monthly nitrate climatology, the North Sea Biogeochemical Climatology (NSBC), and atmospheric data from ERA5 with the aim of quantifying:

- the interannual variability in pre-bloom nitrate concentrations of oceanic surface waters along the NW European shelf edge following deep winter mixing and,
- the magnitude and interannual variability of wind-driven surface Ekman volume and nitrate transport across the shelf edge during the winter months.

The results are discussed in the context of different north-south regimes in deep winter mixing, regional hydrography, nitrate recharge and wind-driven cross-shelf nitrate transport.

2. Methods

2.1. Sector Division Along the NW European Shelf Edge

Shelf edge dynamics and exchange processes across different sectors of the NW European shelf ocean are controlled by a range of physical processes and influenced by regionally variable shelf-break orientation and roughness, hydrographic properties and water mass origins (Huthnance et al., 2022). To investigate the spatial patterns of interannual variability in winter mixing and wind-driven cross-shelf transport, these latitudinally varying characteristics are used to divide the NW European shelf edge into six sectors, numbered 1 to 6 (Figure 1, pink lines). Sector 1 is located at the Armorican Shelf, Sector 2 at the Celtic Sea, Sector 3 at the Porcupine Sea Bight, Sector 4 at Rockall Trough and the Malin Shelf, Sector 5 at the Hebrides shelf, and Sector 6 next to the Faroe-Shetland Channel.

2.2. Nitrate Concentrations on the Shelf

The climatological monthly statistics from the NSBC is used to understand the seasonal and vertical variability of on-shelf nitrate concentrations, as well as their south-to-north variability within the NW European shelf seas. It compiles physical and biogeochemical observations taken across the NW European Shelf between 1960 and 2014 from 8 different data centers, data bases, institutes and regional projects (Hinrichs et al., 2017). The data has a horizontal resolution of $0.25° \times 0.25°$ and 22 vertical levels between the sea surface and 458 m depth. The vertical spacing is 5 m between the surface and 35 m and increases linearly downwards. We used the Level 2 data fields which contain bins occupied by actual observations only.

Mean and standard deviation (SD) of the monthly nitrate climatology were calculated near the surface (0–30 m), bottom (30–200 m) and over all depths (0–200 m). The near-surface and near-bottom locations with available NSBC Level 2 data on each of the shelf sectors (<200 m) are marked by circles and dots separately (Figure S4 in Supporting Information S1). Coastal locations with practical salinity lower than 35 g kg^{-1} are excluded because high riverine nitrate input could heavily bias the sector mean values (see Figure S5 in Supporting Information S1). The number of observations within each sector used to create monthy means are shown in Figure S6 in Supporting Information S1. Among all sectors, the Celtic Sea, Hebrides Shelf, and Faroe-Shetland sectors have the largest numbers of observations during winter. The Porcupine Sea Bight and Rockall-Malin sectors have the smallest number of observations. A monthly nitrate climatology at the Armorican Shelf sector is not available because it is out of the NSBC spatial coverage between 48°N and 65°N.

2.3. Surface Mixed Layer Depth

Monthly mean potential temperature profiles between 2000 and 2021 were obtained from the global, quality controlled EN4 data set (Good et al., 2013). Both the observed, individual subsurface profiles of potential temperature (primarily from ship-based CTD casts and ARGO floats) and the $1° \times 1°$ objective analysis product based on these profiles were extracted.

Time series of monthly surface mixed layer depth (MLD) were created from the objective analysis product for each of the six sectors. Due to large uncertainties in the EN4 salinity estimates, particularly at depths around 200–600 m before 2007, MLD was defined as the depth at which the potential temperature dropped 0.5°C below

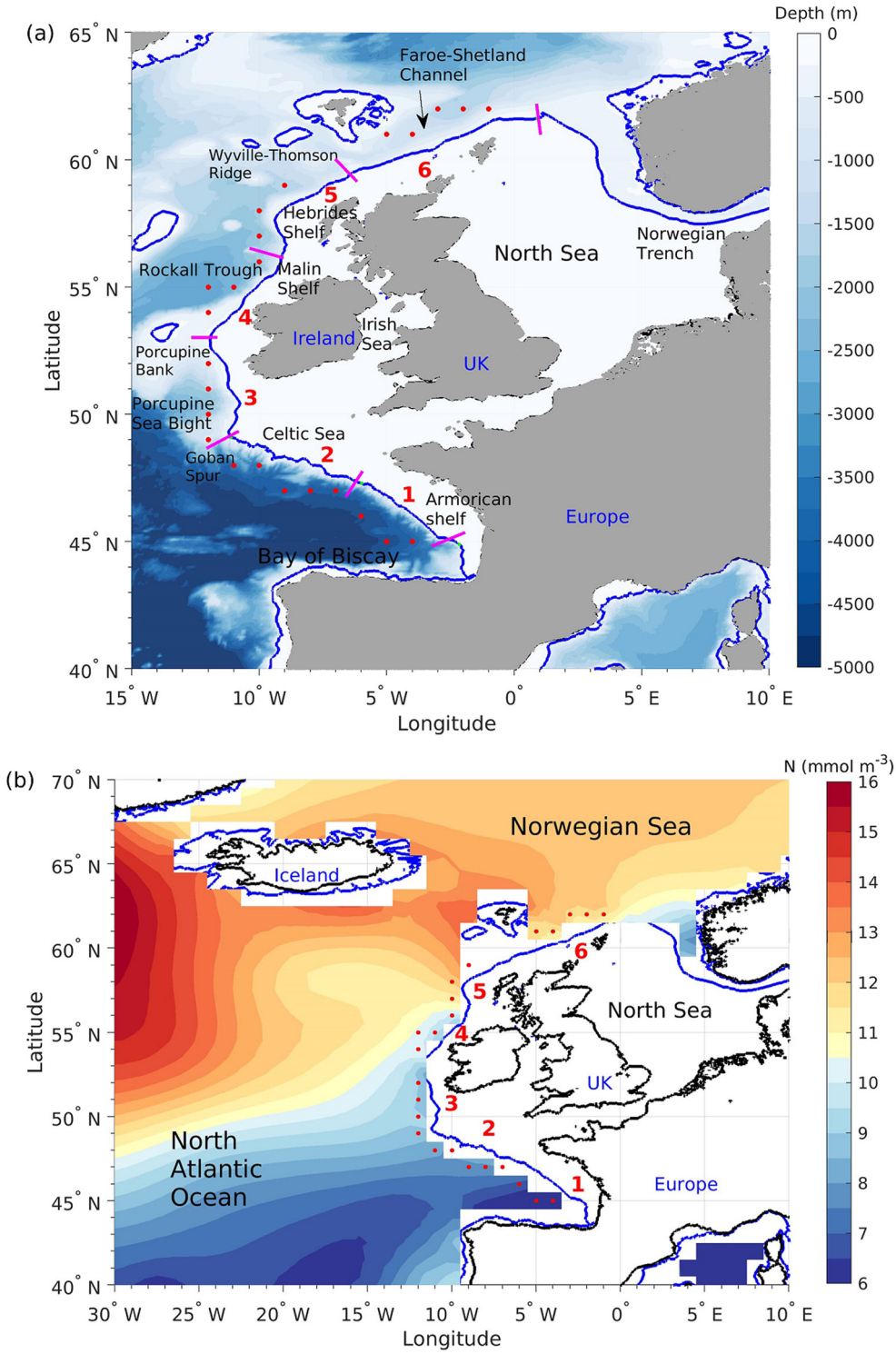

Figure 1. (a) Bathymetry of the North West (NW) European shelf sea and adjacent NE Atlantic ocean. The shelf break is divided into six sectors separated by pink lines. The thick blue contour shows the shelf edge isobath at 200 m. Red dots show locations with EN4 objective analysis data along the shelf edge. (b) Mean nitrate concentration in March at the depth of 200 m in the NE Atlantic Ocean and Norwegian Sea based on World Ocean Atlas data.

the near-surface value (at 15 m), following Johnson et al. (2013). Since the vertical density structure and water column stability along the NW European shelf edge are primarily controlled by temperature and vertical heat exchange with the atmosphere throughout the year, MLD is defined with a temperature threshold as opposed to a density threshold.

Within each sector, EN4 grid points nearest to the shelf break (i.e., 200-m isobath) were selected (Figure 1, red dots) and time series of MLD calculated. These were then averaged to produce a single time series of MLD representative of that sector. To avoid errors and biases associated with the EN4 interpolation of individual profiles from both the shallow shelf and deep ocean onto a coarse 1° grid spanning the shelf break, any objective analysis grid points within 0.5° of the 200 m isobath or with a total water depth <200 m were replaced by the nearest deep ocean location. Points in areas with sharp along-slope bathymetry changes (e.g., Wyville-Thomson Ridge) were also excluded.

To provide confidence in the time series of MLD constructed from the objective analysis product, the MLDs were compared with individual profiles (Figure S1a in Supporting Information S1). The deep-ocean profiles within a 0.5° radius of each grid point were included in the comparison (Figure S1b in Supporting Information S1). Good agreement was found on monthly MLDs in all sectors except near the Faroe-Shetland Channel (Sector 6) where, in some years, the MLD is underestimated by up to 200 m by the objective analysis (Figure S1a in Supporting Information S1). This discrepancy may be related to observational bias toward deeper parts of the Faroe-Shetland Channel where MLD is greater than shallower regions near the shelf break (Figure S1a in Supporting Information S1).

For all sectors, the MLDs based on objective analysis during January-April are on average within 150 m of those based on original profiles collected during the same months. This difference is probably because observations are not always available during the winter and, in the absence of data, the EN4 objective analysis relaxes to a climatology (Good et al., 2013). This means that the strongest mixing events may not always have been captured by direct observations. Additionally, the time series of MLD from original profiles represents a large area around the shelf edge locations, hence accounts for some spatial variability which might also explain some of the differences. Nevertheless, overall the interannual variations of the maximum winter MLD calculated from the objective analysis are in good agreement with those derived from the profile data. Due to the temporal and spatial sparsity of profile data along the NW European shelf break, all MLD analysis in this study is based on the EN4 objective analysis.

2.4. Pre-Bloom Nitrate Concentration at the Shelf Break

The monthly nitrate climatology (1° × 1°) from the WOA 2018 (Boyer et al., 2018) was used to estimate the off-shelf pre-bloom nitrate concentrations within the surface mixed layer that results from the deepest winter mixing each year. We refer to this as the winter mixing recharge of oceanic surface mixed layer nitrate, shortened to "nitrate recharge," which determines the nitrate concentration adjacent to the shelf. To calculate a time series of the annual winter nitrate recharge, the November nitrate profiles was averaged over the maximum depth of winter mixing within each sector. The onset of the increase in surface nitrate concentration with increasing MLD in autumn varies slightly across different sectors (Figure S2 in Supporting Information S1). Near Armorican Shelf, Rockall Trough, Hebrides Shelf, Faroe-Shetland Channel (Sectors 1 and 4–6), surface nitrate starts to increase between September and October. Near the Celtic Sea and Porcupine Sea Bight (Sectors 2 and 3), this increase starts in October-November. For simplicity, the nitrate climatology in November was used to calculate the pre-spring nitrate recharge for all sectors.

The WOA nitrate climatology only covers the upper 800 m of the water column. When the winter MLD was estimated to be deeper than 800 m, the nitrate concentrations were assumed to be equal to those at 800 m. By using the nitrate climatology, any changes associated with interannual variations of the nitrate concentration in the deep nitrate pools, such as those known to occur in the Rockall Trough (Sector 4) due to changes in subtropical versus subpolar water mass proportions (Johnson et al., 2013), were not accounted for. However, due to the sparsity of nitrate data spatially and temporally, particularly for non-summer months, the use of a nitrate climatology was necessary.

2.5. Wind-Driven Ekman Volume and Nitrate Transport

Monthly surface wind stress and direction data were obtained from ERA5 (Hersbach et al., 2020) to calculate wind-driven Ekman transport across the shelf break for each sector. Steady winds result in an Ekman volume

transport 90° clockwise to the wind direction in the northern hemisphere. Assuming the surface Ekman layer is well mixed during winter, the thickness of the surface Ekman layer can be determined by

$$D_{\mathrm{Ek}} = \pi\sqrt{2N_z/f}. \tag{1}$$

Here $f \sim 10^{-4}$ rad s^{-1} is the Coriolis coefficient for the latitude of the NW European shelf. N_z is the vertical eddy viscosity, which is typically $O(10^{-2})$ m^2 s^{-1} or larger within the surface mixed layer (Hahn-Woernle et al., 2014; Martin et al., 2010; Pohlmann, 1996). This yields a D_{Ek} larger than ∼44 m at the ocean surface. The vertically integrated cross-shelf Ekman volume transport in this layer is calculated following:

$$T_{V_{Ek}} = \frac{\tau_w}{\rho_w f} = \frac{\rho_a C_d u_w^2}{\rho_w f}. \tag{2}$$

Here τ_w is the alongshelf wind stress at the ocean surface parallel to the 200-m isobath for each sector, $C_d = \left(0.63 + 0.66\sqrt{u_w^2 + v_w^2} + 0.23\right) \times 10^{-3}$ is the drag coefficient based on Smith and Banke (1975), with u_w and v_w the along-shelf and cross-shelf wind speed, respectively. f is the Coriolis parameter, ρ_w and ρ_a are respectively the density of water and air. The vertically integrated Ekman transport of nitrate within the surface Ekman layer is calculated by

$$T_{N_{Ek}} = \frac{N\tau_w}{\rho_w f}, \tag{3}$$

with N the pre-bloom oceanic nitrate concentration in the surface mixed layer (i.e., nitrate recharge). Positive values of $T_{N_{Ek}}$ and $T_{V_{Ek}}$ indicate on-shelf transport and negative values represent off-shelf transport. Equation 2 shows that surface Ekman transport is approximately quadratically proportional to the wind speed. The mean winter surface Ekman transport was therefore calculated by averaging the monthly Ekman transport over winter months (January-March) before the start of the spring bloom.

Drag of the bottom boundary can result in a similar Ekman layer near the bed and generate a bottom Ekman transport, which is a function of the bottom shear stress (Huthnance et al., 2022). In well-mixed, steady-state conditions, one would expect the surface and bottom Ekman transport to counterbalance each other, especially if there is homogeneity along the shelf break. However, this equilibrium does not happen at a localized level across the NW European shelf (Holt et al., 2009). A balance between the surface and bottom Ekman volume transport within each sector cannot be assumed. Moreover, due to the lack of long-term velocity measurements within the bottom layer at the shelf break, it is challenging to accurately determine the bottom Ekman volume transport or the overall net Ekman transport. Given these constraints, this paper will focus solely on the interannual variations of the surface Ekman transport.

3. Results

3.1. Nitrate Climatology on the Shelves

The mean nitrate concentration on all shelf sectors show strong seasonal variations, which is more pronounced near the surface than near the bottom (comparing blue and red lines in Figure 2). In the Celtic Sea, the near-surface nitrate concentration increases from about 1 mmol m^{-3} in summer to up to 7 mmol m^{-3} in winter. The near-bottom nitrate concentrations, however, ranges between ∼4 and 7 mmol m^{-3} throughout the year. This seasonal variability of the near-surface nitrate concentration is even more pronounced in the northern sectors between Rockall-Malin Shelf and the Faroe-Shetland Channel, where near-surface nitrate concentrations increase from less than 2 mmol m^{-3} in summer to ∼10 mmol m^{-3} in winter. The surface-to-bottom difference in the nitrate concentrations also shows strong seasonal variability. In the summer, nitrate concentrations near the bottom are ∼5–7 mmol m^{-3} higher than those near the surface. During the winter months, the water becomes well-mixed, resulting in nearly vertically homogeneous nitrate concentrations. On all shelf sectors, the depth-averaged nitrate concentration peaks in winter and reaches a minimum in summer (Figures 2a–2e, orange error bars). This highlights that vertical mixing and biological recycling within the bottom layer cannot sufficiently replenish the net drawdown of nitrate during the spring-autumn period or losses to benthic denitrification. Therefore, external sources, such as oceanic nitrate, are required to replenish the nitrate levels on the shelf.

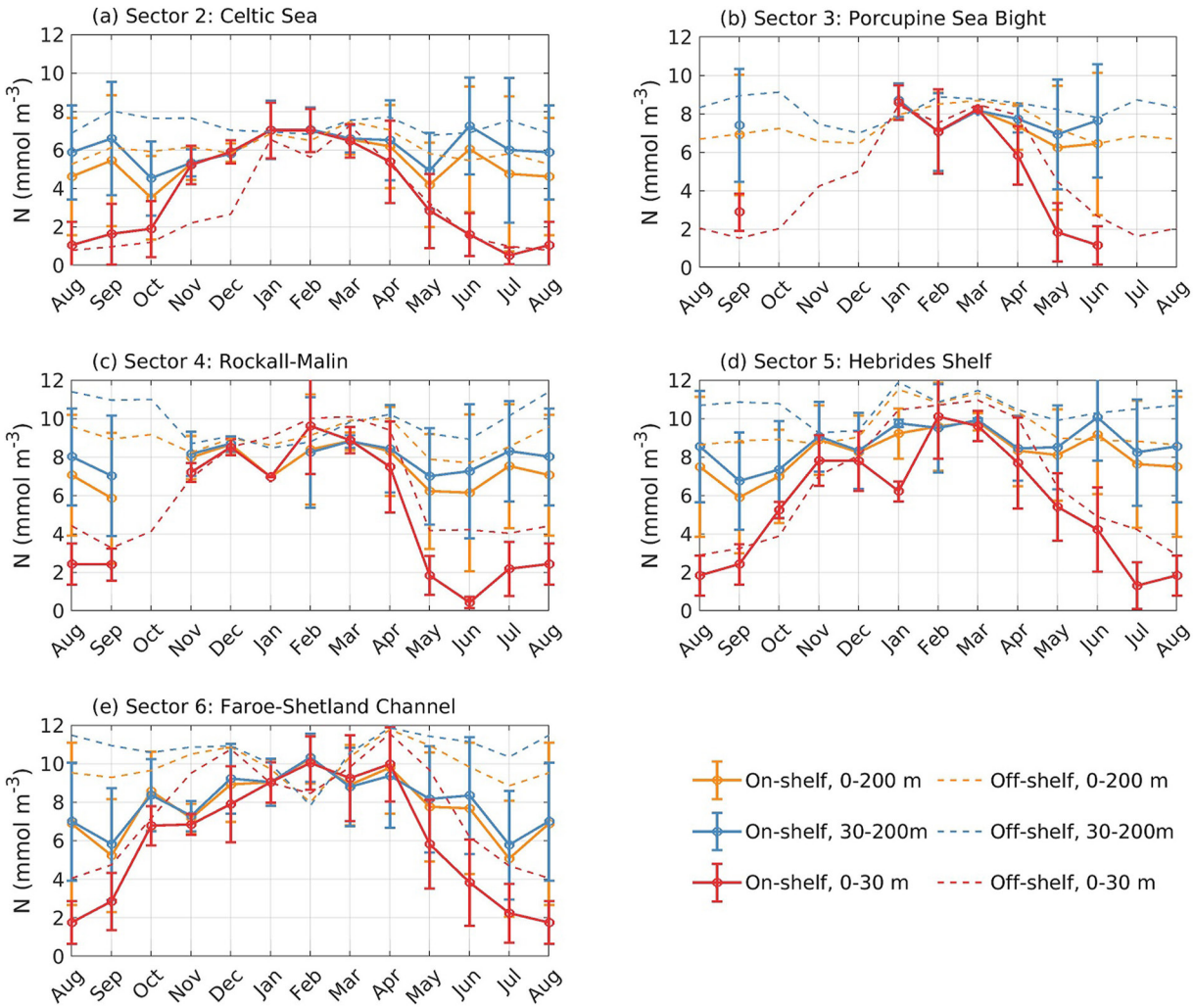

Figure 2. Monthly means and standard deviations of the near-surface (0–30 m depth, red error bars), bottom (30–200 m, blue error bars) and depth averaged (0–200 m, orange error bars) nitrate concentration for each on-shelf sector, derived from the North Sea Biogeochemical Climatology. Red, blue, and orange dashed lines show the off-shelf nitrate concentrations averaged over 0–30, 30–200, and 0–200 m for each of the off-shelf sectors, derived from the World Ocean Atlas 2018.

The winter surface nitrate concentration difference between on-shelf and off-shelf locations also exhibits notable variations from south to north, as illustrated in Figure 2 by the comparison between red error bars and red dashed lines. In the Celtic Sea, the averaged off-shelf near-surface nitrate concentration is ∼1–2 mmol m^{-3} lower than the on-shelf nitrate concentration in January-February, and ∼1 mmol m^{-3} higher than the on-shelf value in March. In the northern sectors between Rockall-Malin and Hebrides shelves, however, the averaged off-shelf near-surface nitrate concentration is about 2–4 mmol m^{-3} larger than that on the shelf over January-March (Figures 2c–2e). Such cross-shelf nitrate gradient is essential for advective and/or diffusive processes to contribute to the cross-shelf nitrate exchange within the surface layers. Below 30 m, off-shelf nitrate concentrations are close to or higher than on-shelf values in all sectors (comparing blue dashed lines with blue error bars, Figure 2).

3.2. Interannual Variability of Oceanic Winter Mixed Layer Depth

In all shelf edge sectors, the MLD shows clear seasonal variability, with shallowing in summer and deepening in winter. The annual maximum MLD also varies significantly between sectors along the shelf break: it increases from ∼150 m off the Armorican Shelf to more than 900 m near Malin Shelf, decreasing to 200–300 m at the Faroe-Shetland Channel (Figure 3a). Within each sector the depth of the maximum winter mixing shows strong interannual variations, the range of which decreases with increasing latitude (Figure 3b). At the southernmost sector, along the Armorican shelf boundary, the maximum MLD varies between 150 m in 2002 and 600 m in

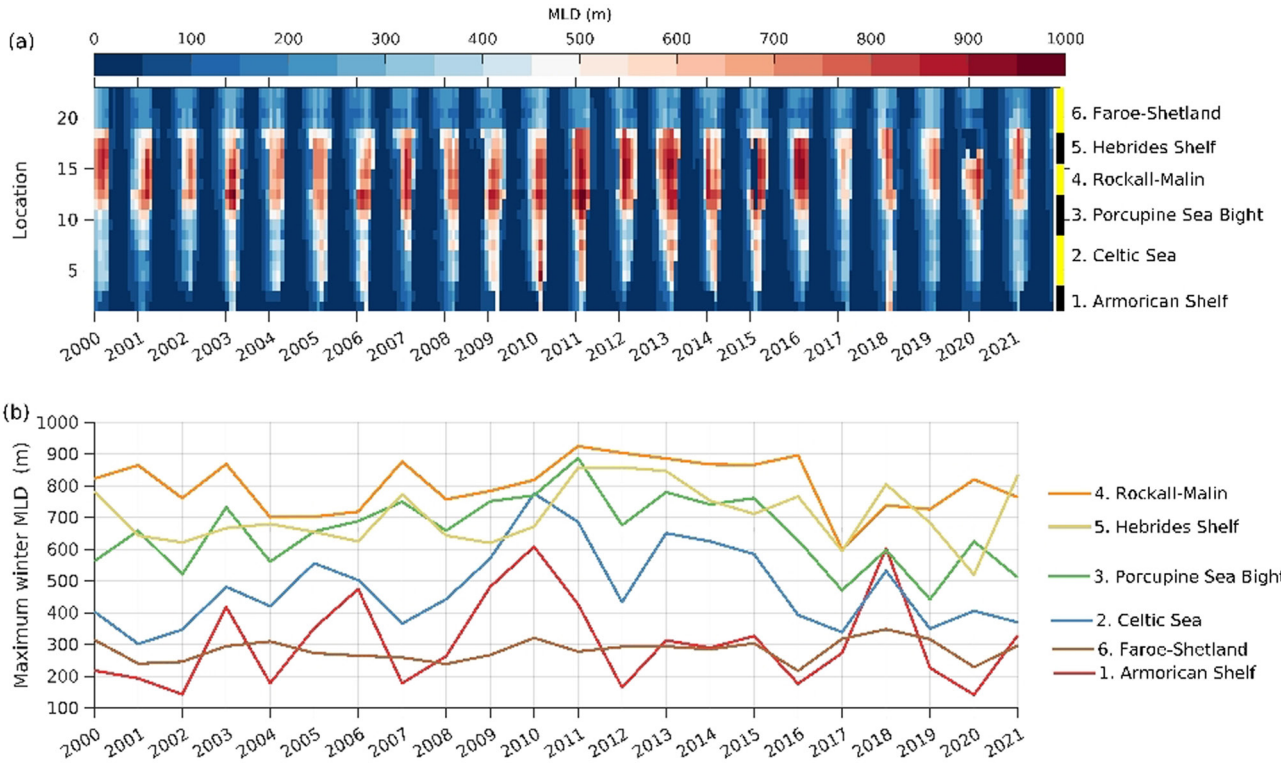

Figure 3. (a) Monthly variations of mixed layer depth (MLD) at all selected locations (red dots in Figure 1) along the North West European shelf break. The yellow-black line marks locations within each shelf sector. (b) Interannual variations of the maximum winter MLD for each sector.

2010, a range of 450 m. In contrast, in Sector 6, Faroe-Shetland, the maximum MLD only varies by ~100 m, from 200 to 300 m between years. There are also differences in the MLD within each of the sectors. The largest SD is found in the Porcupine Sea Bight (240 m) in 2003, and the smallest SD in the Faroe-Shetland Channel with the period average SD of ~26 m.

3.3. Shelf Edge Temperature, Salinity and Nitrate

The nitrate concentration at the shelf break shows strong seasonal variations in all sectors (Figure 4a, shaded color). The surface nitrate concentration peaks between February-April, reaches its minimum in summer, and increases again from autumn. This coincides with the seasonal shallowing/deepening of the surface mixed layer (Figure 4a, black lines), confirming the importance of seasonal deepening of the surface mixed layer to nitrate concentrations in the ocean surface. Nitrate depletion in the sunlit surface waters due to phytoplankton growth also contributes to the seasonal variations of surface nitrate concentration and increases the vertical nitrate gradients in spring and summer (Omand & Mahadevan, 2015). The winter nitrate concentration around the range of maximum winter MLD fluctuations during 2000–2021 also varies among different shelf-break sectors (Figure 4a, blue bars).

There are clear north-south differences in the water masses along the shelf break, with a transition from warmer, saltier subtropical origin water with lower nitrate concentrations in the south, to increasing proportions of colder, fresher, nitrate-rich subpolar origin water further north (Figures 4b–4d). Between the Armorican and Hebrides shelves (Sectors 1–5), the upper water mass just below the surface mixed layer is Eastern North Atlantic Water (ENAW), although its properties vary latitudinally. Below this, Mediterranean Overflow Water (MOW) is clearly seen in Sector 1 and 2 and less clearly in Sectors 3 and 4. Although the core of MOW is around 1,000 m, the influence of its high nitrate concentrations can be seen at 600 m. The water masses in the Faroe-Shetland channel (Sector 6) are different from those in Sectors 1–5, reflecting both the Atlantic and Arctic influences on this area. Two upper water masses are seen: ENAW which enters the Faroe-Shetland Channel from the south, and the slightly denser Modified North Atlantic Water which enters the region from the north. Below these upper water masses is Modified Eastern Icelandic Water which also enters from the north.

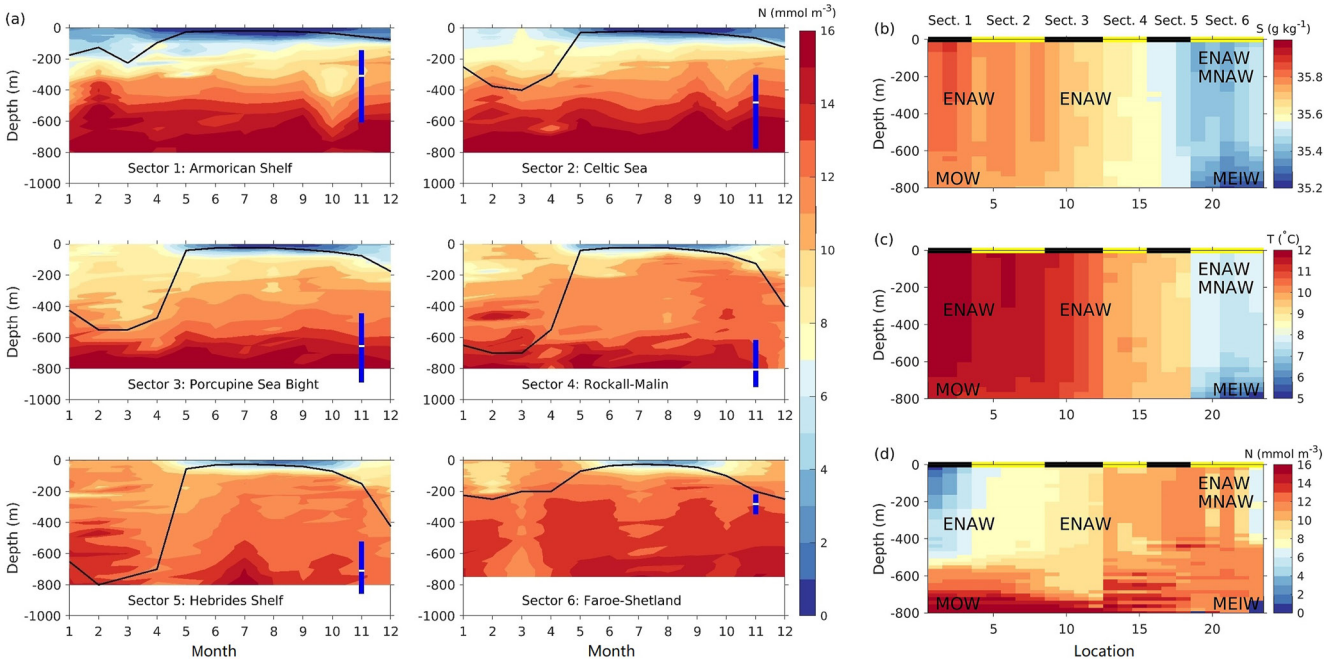

Figure 4. (a) Annual cycle of variability in the vertical nitrate distribution for each sector based on the World Ocean Atlas monthly nitrate climatology. Black lines mark the mixed layer depth (MLD) based on the monthly temperature climatology. Vertical blue bars represent the range in the maximum MLDs experienced during the winter months between 2000 and 2021 calculated from EN4 (b–d) Vertical distribution of absolute salinity, potential temperature, and nitrate (from the March climatology) along the North West European shelf break. The yellow-black line marks locations within each shelf sector. Dominant water masses along the shelf break are labeled in (b–d) including the Eastern North Atlantic Water, Mediterranean Overflow Water, Modified North Atlantic Water, and the Modified Eastern Icelandic Water.

3.4. Interannual Variability in Oceanic Pre-Bloom Nitrate Concentration

Due to different dominant water masses, the pre-bloom nitrate concentration within the surface mixed layer along the NW European shelf break varies between sectors. The winter nitrate concentrations around the typical winter MLDs (Figure 4a, blue bars) in the northern sectors are larger than those in the southern sectors. As a result, the pre-bloom oceanic nitrate recharge that results from deep winter mixing adjacent to the shelf is higher in the northern sectors than further south in most years (Figure 5a). The recharged nitrate concentration varies from more than 10.5 mmol m^{-3} between Rockall-Malin and the Faroe-Shetland sectors to 3.9–9.8 mmol m^{-3} off the Armorican Shelf.

The magnitude of interannual variability in winter nitrate recharge at the shelf boundary also varies with latitude. The largest changes between years occur adjacent to the Armorican Shelf and Celtic Sea (by ~6 mmol m^{-3} from 2018 to 2020). North of the Porcupine Sea Bight, the interannual variability is less than 1 mmol m^{-3}. The weak temporal variability in the winter nitrate recharge in the Rockall-Malin and Hebrides sectors is in contrast to the moderate interannual variability of maximum winter MLD (Figure 5b, blue line). This is partly related to the weak vertical gradients of nitrate concentration in November near the maximum winter MLD and partly caused by the lack of nitrate data below 800 m (Figure 4a).

The mean vertical gradient of nitrate concentration within the range of maximum winter MLD fluctuations is weakest in the Hebrides and Faroe-Shetland sectors (Figure 5b, brown line). As a result, interannual variations of maximum winter MLDs have little impact on the interannual variability of winter nitrate recharge in these sectors. The more variable nitrate recharge in the southern Sectors 1 and 2 (i.e., Armorican Shelf, Celtic Sea) compared to further north is associated with large interannual MLD variability (Figure 3b) and strong vertical nitrate gradients near the maximum winter MLDs (Figure 5b). South of 50°N, the high nitrate signature of MOW is present at around 600 m depth and therefore accessible during years with particularly deep winter mixing (e.g., 2010, 2018). Since nitrate concentration changes substantially within the range of MLD fluctuations in the southern sectors (Figure 4a), small changes in the depth of winter mixing can lead to large year-to-year variations of winter nitrate recharge. The winter nitrate recharge averaged over 2000–2021 is close to the March climatology

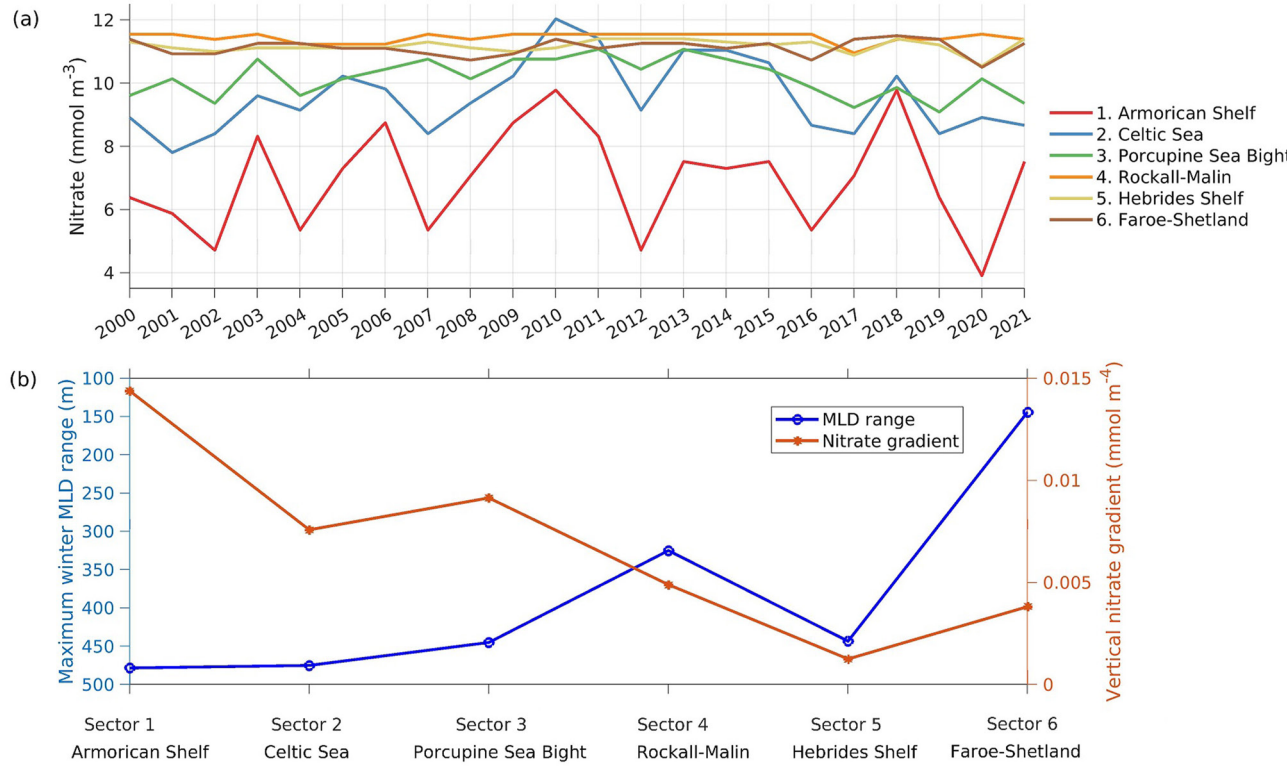

Figure 5. (a) Recharged oceanic nitrate concentration for all sectors following the deepest winter mixed layer of each year. (b) Mean vertical nitrate gradient within the depth range of the winter mixed layer (brown line). This is calculated by dividing the maximum difference in the nitrate concentration within the maximum winter mixed layer depth (MLD) range over the maximum magnitude of the interannual variation of the maximum winter MLD (blue line).

of surface nitrate (top 30 m, Figure S2 in Supporting Information S1) along the NW European shelf break except in Sectors 1, 2, and 3, where the estimated pre-bloom nitrate concentration is over 1 mmol m^{-3} larger than the climatology, respectively. This might be due to the overestimated maximum winter MLD in these sectors based on the EN4 objective analysis when compared to the values obtained from the original observations (Figure S1a in Supporting Information S1).

To assess any potential biases introduced by our methodology and to provide confidence in our results, we compared the estimated winter MLDs and nitrate recharge with the limited number of published observational time series available. Interannual variations of the maximum winter MLD and winter nitrate recharge between 2003 and 2010 at the Armorican Shelf break (Sector 1, Figure 5a) are in good agreement with observations made in the Bay of Biscay during this period (Hartman et al., 2014). We did not find any nitrate observations close to Sector 2 or 3 within the present study period (2000–2021). Nevertheless, the estimated MLD (300 m) and winter nitrate recharge (~8 mmol m^{-3}) near the Celtic Sea shelf break (Sector 2) in 2001 is close to the observations near the Gorban Spur measured between January and February in 1993, when the surface mixed layer was also 300 m (Hydes et al., 2001). Moreover, Hartman et al. (2010) observed that the surface nitrate concentration near the Porcupine Abyssal Plain observatory (more than 0.7° west of our Sectors 2 and 3) varied between 4.9 and 8.3 mmol m^{-3} from 2003 to 2005. Near Sectors 4 and 5, winter nitrate concentrations within the upper waters (200–700 m) at the Extended Ellett Line latitude (57.5°N) varied between 10.5 and 12.5 μM during 2000–2010 (Johnson et al., 2013). These observed interannual variations in the winter nitrate concentrations are both close to those estimated in the current study.

3.5. Interannual Variability of Cross-Shelf Wind-Driven Ekman Transport

To investigate the contribution of wind-driven surface Ekman transport to the oceanic nitrate supply to the adjacent shelf sea, the Ekman volume and nitrate transport integrated over the surface Ekman layer were calculated for each shelf-edge location and sector. The monthly surface Ekman volume transport, $T_{V_{Ek}}$, along the NW

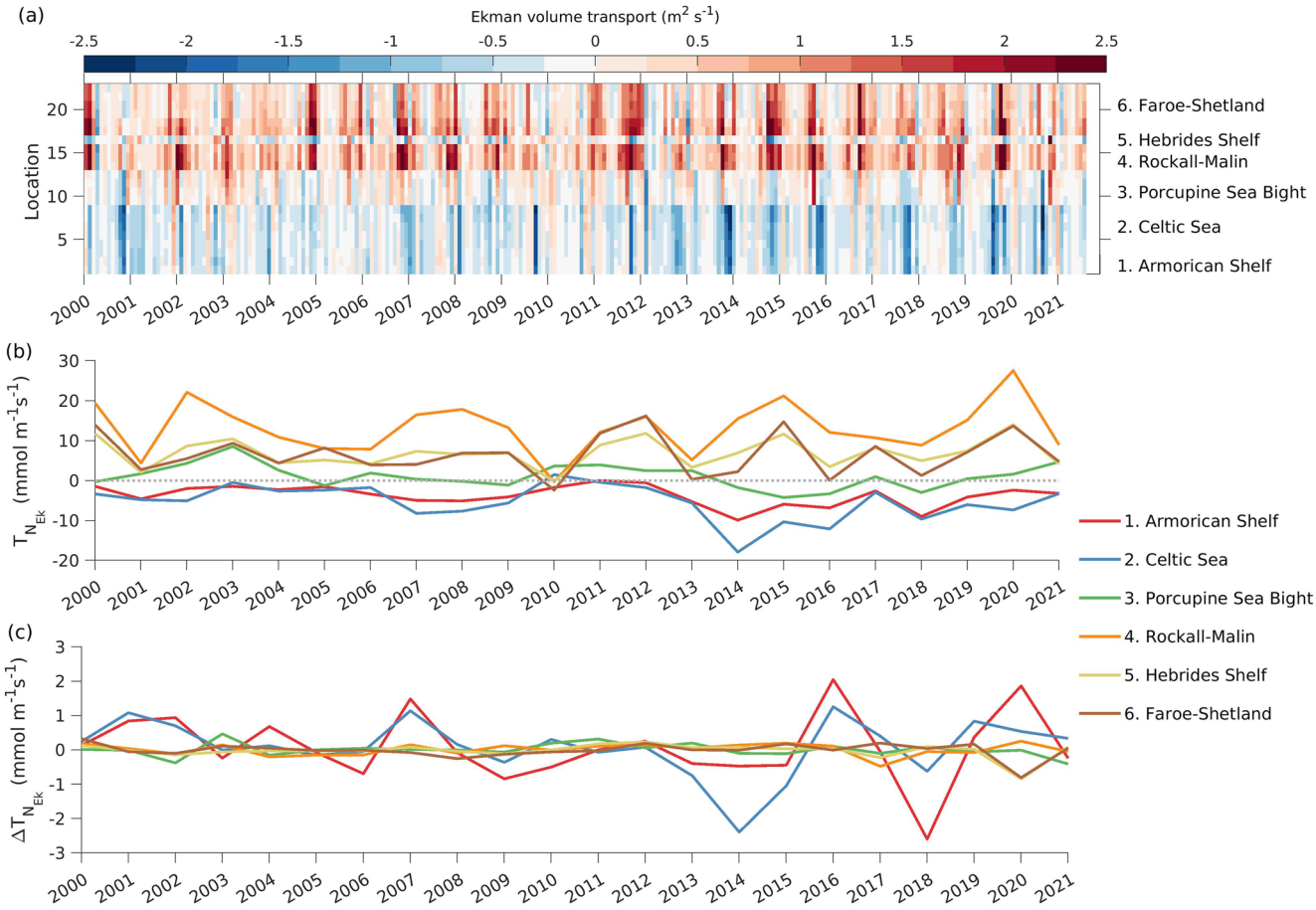

Figure 6. (a) Monthly surface Ekman volume transport across the North West European shelf break, $T_{V_{Ek}}$, at all shelf-edge locations (Figure 1, red dots) during the period of 2000–2021. (b) Sector-mean winter Ekman transport of nitrate $\left(T_{N_{Ek}}\right)$ averaged over January-March (solid lines), calculated using the interannually varying pre-bloom oceanic nitrate recharge shown in Figure 5a. Dashed lines show $T_{N_{Ek}}$ calculated using the 2000–2021 sector average nitrate recharge, thereby removing variability driven by interannual variations of the maximum winter mixed layer depth. Positive values of $T_{V_{Ek}}$ and $T_{N_{Ek}}$ denote on-shelf transport and negative values off-shelf transport. (c) Difference in surface Ekman nitrate transport $\left(\Delta T_{N_{Ek}}\right)$ between values factoring in interannual variations of nitrate recharge versus those based on the pre-bloom surface nitrate concentration averaged over the period of 2000–2021.

European shelf break is seasonally variable with the largest on-shelf/off-shelf transport in winter for all shelf-edge locations (Figure 6a). Contrasting patterns of $T_{V_{Ek}}$ are observed in different sectors of the NW European shelf break. During winter, $T_{V_{Ek}}$ is mostly off-shelf near the Armorican Shelf and Celtic Sea (negative values, Sectors 1 and 2), and on-shelf within the Rockall-Malin, Hebrides and Faroe-Shetland sectors (positive values, Sectors 4–6). The direction of $T_{V_{Ek}}$ at the Armorican Shelf break (Sector 1) agrees with recent studies by Ricker and Stanev (2020) and Huthnance et al. (2022), who also found wind-driven off-shelf particle transfer from the Armorican Shelf to Bay of Biscay. Near Porcupine Sea Bight (Sector 3), the direction of Ekman transport across the shelf break is more variable than in Sectors 1–2.

The winter North Atlantic Oscillation index was positive for most years between 2000 and 2021, when the Northern Europe is dominated by strongly westerly winds (Koul et al., 2019; Rodrigo, 2021). The above-mentioned north-south contrast in the direction of $T_{V_{Ek}}$ across the NW European Shelf edge is therefore associated with the shelf-break orientation, which shifts from southeast-to-northwest in Sectors 1 and 2 to south-to-north in Sector 3, and southwest-to-northeast in Sectors 4–6. During spring-summer, $T_{V_{Ek}}$ results in frequent ocean water import in Sectors 1 and 2 to the adjacent shelf seas due to downwelling favorable winds, even though the magnitude is generally smaller than the winter off-shelf transport. In Sector 3, $T_{V_{Ek}}$ also contributes to an oceanic water import during spring-summer of most years, which is more frequent and stronger compared to that in Sectors 1 and 2. In the northern Sectors 4–6, $T_{V_{Ek}}$ tends to import ocean water to the shelf seas throughout most of the study period due to upwelling favorable winds.

The winter surface Ekman nitrate transport $\left(T_{N_{Ek}}\right)$ across the NW European shelf break, averaged over January-March, varies significantly with latitude (Figure 6b). The magnitude of $T_{N_{Ek}}$ reaches its maximum near Malin Shelf and Rockall Trough (up to 27.5 mmol m^{-1} s^{-1}, onto the shelf) and is a minimum along the Armorican Shelf (less than 9.9 mmol m^{-1} s^{-1}, off the shelf). In the north, along the Rockall-Malin and Hebrides sectors (Sectors 4–5), $T_{N_{Ek}}$ is on-shelf with a period-average value during 2000–2021 of 13.1 and 6.9 mmol m^{-1} s^{-1}, respectively. In the south, $T_{N_{Ek}}$ is off-shelf with an averaged value of 3.7 mmol m^{-1} s^{-1} across the Armorican Shelf (Sector 1) and 5.4 mmol m^{-1} s^{-1} near the Celtic Sea (Sector 2). The spatial pattern of $T_{N_{Ek}}$ contrasts with the spatial variability in the pre-bloom nitrate concentration, which monotonically increases from Armorican Shelf (Sector 1) to Rockall-Malin Shelf (Sector 4). This contrast can be explained by the relationship between $T_{N_{Ek}}$ and the cross-shelf volume transport, which is determined by the along-shelf wind stress (τ_w). Since the spatial and temporal variations of τ_w are typically larger than the pre-bloom nitrate concentration, variability of $T_{N_{Ek}}$ is dominated by the Ekman volume transport rather than year-to-year differences in the nitrate recharge.

Whilst the magnitude of $T_{N_{Ek}}$ is to first order controlled by the cross-shelf volume transport, and typically unaffected by year-to-year differences in the winter nitrate recharge, in the southern sectors there are a few years where the depth of winter mixing may have been important (Figure 6c). Negative values of $\Delta T_{N_{Ek}}$ in the Armorican and Celtic Sea sectors in 2018 and 2014 respectively suggest that deeper than average winter mixing, and therefore higher than average nitrate recharge, was responsible for up to 2–3 mmol m^{-1} s^{-1} of the total wind driven off-shelf nitrate transport in those years. In 2001, 2002, 2007, 2016, and 2020, both the Celtic and Armorican sectors experienced shallower than average winter mixing and therefore lower nitrate recharge concentrations, which reduced the magnitude of $T_{N_{Ek}}$ by 1–2 mmol m^{-1} s^{-1}. This interannual variability in the oceanic nitrate recharge makes less than ~50% contribution to the total magnitude of $T_{N_{Ek}}$ in most years. Nevertheless, in the winter of 2020 the low nitrate recharge following shallow winter mixing (MLD ≤150 m) accounts for 78% of the small magnitude of $T_{N_{Ek}}$ (2.4 mmol m^{-1} s^{-1}) in the Armorican Shelf sector. It is noticeable that this does not happen in the northern sectors.

4. Discussion

4.1. Latitude Dependent Cross-Shelf Transport Regimes

Our results have shown clear latitudinal differences in the winter surface cross-shelf Ekman transport of nitrate following deep winter mixing and nitrate recharge along the NW European shelf edge, as summarized in Figure 7a. In the north, the winter averaged $T_{N_{Ek}}$ is on-shelf: 13.1 mmol m^{-1} s^{-1} in the Rockall-Malin sector and 6.9 mmol m^{-1} s^{-1} in the Hebrides sector. In the south, $T_{N_{Ek}}$ is off-shelf with an averaged value of 3.7–5.4 mmol m^{-1} s^{-1} between the Armorican and Celtic sectors. In addition to wind stress, the south-to-north differences in the magnitude and direction of $T_{N_{Ek}}$ are also related to the differences in the shelf-break orientation and the ocean nitrate recharge following the deepest winter mixing near the shelf break.

Even though previous sections have focused on the surface Ekman transport (solid green and blue arrows in Figures 7b and 7c), the net cross-shelf Ekman transport also depends on the bottom Ekman transport (not quantified here, see dashed arrows in Figures 7b and 7c). Contributions of these two components to the net cross-shelf nitrate exchange are controlled by the vertical nitrate gradients on the outer shelves (at <200 m) and the cross-shelf nitrate gradients (N_x). Since this study focuses on winter months when the shelf water column and vertical nitrate profile are fully mixed, the net winter cross-shelf Ekman nitrate transport depends more on cross-shelf nitrate gradients than vertical gradients. In the northern shelf Sectors (i.e., Rockall-Malin, Hebrides Shelf), the winter nitrate concentrations at the shelf break are clearly higher than those on the adjacent shelves, whereas the surface-to-bottom differences in the on-shelf winter nitrate concentration are minor (Figures 2c and 2d). Since the winter winds along these sectors are downwelling favorable, both the bottom Ekman transport, which flushes the nitrate-lower shelf water to the ocean, and the surface Ekman transport, which brings the nitrate-rich oceanic water onto the shelf, act to supply oceanic nitrate to support the shelf spring bloom (Figure 7b, green arrows). In the southern sectors (e.g., Celtic Sea), the averaged winter nitrate concentrations near the surface are higher on the shelf than those off the shelf (Figure 2a). Although not extensively observed in the bottom layers (Figure S6a in Supporting Information S1), the winter cross-shelf nitrate gradients near the bottom are expected to resemble those near the surface due to the well-mixed water column. As the winter winds are mostly upwelling favorable along the southern sectors, the surface Ekman transport (Figure 7c, solid blue arrow) acts to export nitrate out of the shelf.

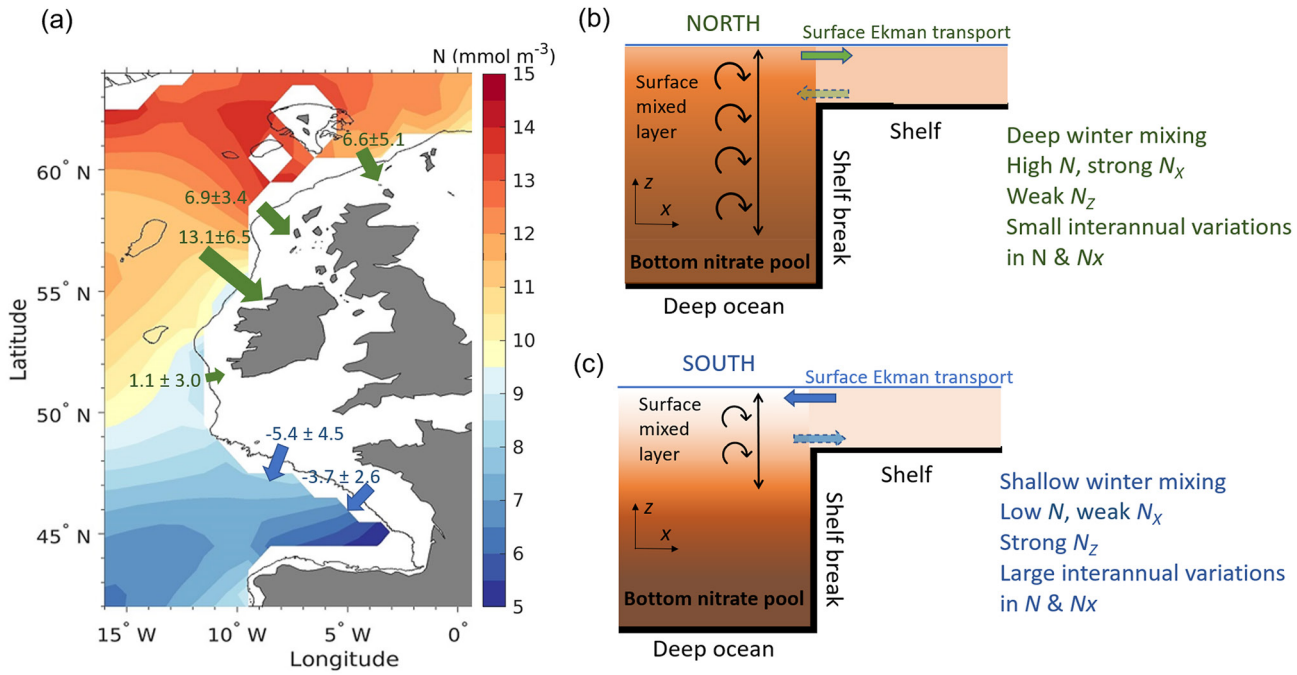

Figure 7. (a) Latitude-dependent regimes in the winter cross-shelf surface Ekman nitrate transport $\left(T_{N_{Ek}}\right)$ following the maximum ocean nitrate recharge along the North West European Shelf edge. Arrows indicate the direction and magnitudes (mean and standard deviations) of $T_{N_{Ek}}$ for each sector (2000–2021). The March nitrate climatology at 200 m depth from the World Ocean Atlas is shaded and the 200 m isobath contoured in black. (b, c) Schematic diagrams showing two different winter cross-shelf nitrate transport regimes in the north (Rockall-Malin and Hebrides shelves) and south (Armorican Shelf and Celtic Sea).

We also identified two winter cross-shelf nitrate transport regimes respectively for the north and the south associated with the winter nitrate recharge at the shelf break (Figures 7b and 7c). Due to shallower winter mixing in the south compared to the north (Figure 3) and a higher proportion of subtropical origin water, the off-shelf and on-shelf winter nitrate concentrations (N) are higher in the north than in the south (Figure 2). Apart from the south-to-north shift in the sign of cross-shelf nitrate gradient, the magnitude of cross-shelf nitrate gradients seems to also increase monotonically with latitude. As shown in Figure 2, difference between the on-shelf and off-shelf winter-averaged (January-March) nitrate concentration increased from less than 1 mmol m^{-3} in the south sectors (e.g., Celtic Sea) to more than 2 mmol m^{-3} in the north (e.g., Rockall-Malin, Hebrides). This spatial variability in the winter cross-shelf nitrate gradients suggest that cross-shelf exchange processes, (e.g., advective and diffusive processes), are likely to make a larger contribution to the pre-spring shelf surface nitrate supply in the north compared to the south.

In the north, due to weak vertical nitrate gradients (N_z) within the depth range of maximum winter mixing, interannual variability in the depth of the winter MLD only slightly affects the interannual variations of the pre-bloom ocean nitrate recharge and cross-shelf nitrate transport (Figure 7b). Nevertheless, due to high N and strong N_x following the deepest winter mixing, advective and/or diffusive ocean-shelf exchange processes (e.g., Ekman transport, eddy transport) can contribute significantly to the total pre-bloom nitrate supply to the northern shelves. In the south, N_z is large before winter mixing, strong interannual variability in the deepest winter mixing can therefore result in large interannual variations of N and N_x near the shelf break (Figure 7c). However, the overall pre-bloom oceanic nitrate supply to the southern shelves is limited by low N and weak (negative) N_x.

The cross-shelf transport regimes suggest that interannual variability of the winter oceanic nitrate supply to the shelf depends not only on the strength/direction of winter winds, but also the deepest winter mixing and the vertical nitrate distributions in the ocean nitrate pools near the shelf edge. Therefore, future changes in winter atmospheric and ocean conditions (e.g., winds, storms, subsurface temperature, water masses) due to, for example, a poleward shift in the North Atlantic eddy-driven jet stream (Woollings & Blackburn, 2012) and/or changes in the strength and position of the Subpolar Gyre (Clark et al., 2022), could modulate the importance of winter oceanic nitrate supply to spring bloom in shelf seas.

4.2. Pre-Bloom Nitrate Concentration Changes on the Northern Shelves

In the Hebrides Shelf and Rockall-Malin sectors, 62% of the surface waters originate in the Atlantic Ocean during prevailing westerly wind conditions (Jones et al., 2018). Over the winter months, the shelf nitrate pool in these sectors increases by ~1–2 mmol m^{-3} (Figures 2c and 2d, orange solid lines). In this section, we attempted to quantify the contribution of winter on-shelf surface Ekman transport to the pre-bloom increase in shelf nitrate concentration (ΔN) for these sectors.

By assuming a constant cross-shelf nitrate gradient near the shelf break during the winter months, we can estimate an upper bound of ΔN driven by the on-shelf winter surface Ekman transport:

$$\Delta N = \frac{\int T_{V_{Ek}}(N_{off} - N_{on})dt}{BD_{shelf}}. \quad (4)$$

Here, $D_{shelf} \sim 100$ m is the averaged water depth of the outer shelves. B is the width of the outer shelf, which is ~50 km in Sector 4 (Rockall-Malin, orange arrow in Figure S4 in Supporting Information S1) and 100 km in Sector 5 (Hebrides Shelf). $T_{V_{Ek}}$ is the cross-shelf winter surface Ekman transport. N_{on} and N_{off} are the on-shelf and off-shelf nitrate concentrations during the winter months, respectively. Comparing the on-shelf (NSBC) and off-shelf (WOA) nitrate climatology allows a rough estimate of the winter cross-shelf nitrate difference on the Rockall-Malin and Hebrides shelves (Figures 2c and 2d), with $N_{off} - N_{on} \approx 2$ mmol m^{-3}.

Integrating the surface Ekman transport across the Rockall-Malin Shelf (Sector 4) for the period from February to April, as explained in the following paragraph, results in a 1.1 mmol m^{-3} increase in the nitrate concentration within the mixed shelf water column averaged between 2000 and 2021 ($T_{V_{Ek}} = 0.7$ m^2 s^{-1}). On the Hebrides Shelf (Sector 5), the average winter surface Ekman transport ($T_{V_{Ek}} = 0.4$ m^2 s^{-1}) results in a smaller increase in the nitrate concentration: $\Delta N = 0.6$ mmol m^{-3}. These estimates suggest that winter surface Ekman transport may contribute to more than 50% of the pre-bloom nitrate recharge in these sectors. However, these estimates do not account for any changes in the cross-shelf nitrate gradients during these 3 months, nor do they include nitrate losses through off-shelf drainage in the bottom Ekman layer or from sedimentary denitrification. They should therefore be considered an upper limit on the possible increase in the shelf nitrate pool over the winter months driven by the surface Ekman transport.

Equation 4 suggests that the prebloom surface Ekman transport of nitrate onto the shelf depends strongly on the difference between the on-shelf (N_{on}) and off-shelf (N_{off}) nitrate concentrations established following the deepest winter mixing. Hence, the overall contribution of the winter surface Ekman transport to the prebloom on-shelf nitrate supply can vary significantly with the timing of the maximum winter MLD and the timing of the onset of strong stratification in spring. These timings determine when cross-shelf nitrate gradients are strongest and cross-shelf transport most effective compared to vertical mixing processes (e.g., internal waves). Between the Malin-Hebrides sectors (Sectors 4–5), the nitrate concentrations in surface waters reach the maximum between February and March (Figures 2c and 2d), and the sharpest decreases of N occur in April. Hence, we deduce that surface Ekman transport during February-April may be of most relevance to the pre-bloom cross-shelf nitrate transport in these sectors.

4.3. Limitations

Our study identifies clear latitudinal differences in the magnitude, direction and interannual variability of the winter wind-driven cross-shelf transport along the NW European shelf. Nevertheless, several limitations exist in the quantification of the winter surface MLD, nitrate recharge, and their possible contributions to the prebloom on-shelf nitrate supply. These limitations are associated with limited data availability, for example, subsurface temperature and nitrate concentrations near the shelf break during winter, and nitrate concentrations on the shelf during winter-spring.

Moreover, whilst spring primary production in shelf seas requires oceanic origin nutrient transport onto the inner shelf regions, the annual shelf nutrient budget and the magnitude of the spring bloom are sensitive to other biological and physical processes on the shelf (e.g., nutrient recycling, internal tides, bottom Ekman transport), which are not considered in this study. Between the Armorican Shelf and Bay of Biscay, for example, eddies play an important role in the cross-shelf exchange (Akpınar et al., 2020; Porter et al., 2016), particularly at mid-depths.

In the central Celtic Sea, where 90% of the nitrate pool is estimated to be of oceanic origin, in March 2015 only 25% was considered to have been recently supplied; up to 62% was accounted for by recycling of organic nitrogen (Ruiz-Castillo et al., 2019). Near the Faroe-Shetland Channel, winter nitrate concentration strongly corresponds with the local wind direction (Pätsch et al., 2020), which is not considered here by using the nitrate climatology.

5. Conclusions

Nutrient availability at the start of the spring phytoplankton bloom in temperate shelf seas is an important control on the magnitude of spring primary production, which varies between years. Based on an objective analyses of subsurface ocean temperatures, a nitrate climatology, and an atmosphere reanalysis product, we investigated interannual variations of the pre-bloom oceanic nitrate concentration following deep winter mixing (i.e., nitrate recharge) along the NW European shelf edge and the wind-driven cross-shelf Ekman nitrate transport.

We found clear differences between the northern and southern sectors in the magnitude and interannual variability of both the depth of maximum winter mixing and nitrate recharge. The maximum depth of winter mixing increases between the Armorican Shelf in the south (~150–600 m) and Rockall-Malin sector further north (~600–900 m). North of the Wyville Thomson Ridge, in the Faroe-Shetland sector the winter MLD is shallower (~200–300 m). This south-to-north difference results in smaller winter ocean nitrate recharge in the southern sectors (Armorican Shelf, Celtic Sea) than that in the north (Rockall-Malin and Hebrides shelves). However, the interannual variations in the maximum winter MLD, as well as the vertical nitrate gradients within the range of maximum MLDs, are much larger in the south than further north. For this reason, the interannual variability in the ocean nitrate recharge and cross-shelf nitrate gradients near the shelf break are substantially larger in the south compared to the north.

The magnitude and direction of the winter cross-shelf surface Ekman nitrate transport also strongly depend on the latitude as a result of the south-to-north differences in the shelf break orientation. The winter surface Ekman nitrate transport in the southern sectors is off-shelf (average ~3.7–5.4 mmol m^{-1} s^{-1}). Near Porcupine Sea Bight, the surface Ekman transport changes from on-shelf to off-shelf from year to year (average 1.1 mmol m^{-1} s^{-1}). In the north, near Rockall-Malin and Hebrides shelves, the on-shelf surface Ekman nitrate transport is the largest among all sectors (6.9–13.1 mmol m^{-1} s^{-1}). Near the Faroe-Shetland channel, the averaged on-shelf winter surface Ekman transport is 6.6 mmol m^{-1} s^{-1}.

Our study reveals large spatial and interannual variability in the contributions of winter mixing and wind-driven cross-shelf Ekman nitrate transport to the interannual variability in the pre-bloom oceanic nitrate supply to temperate shelf seas. This implies that the maximum winter mixing and cross-shelf nitrate gradients near the shelf edge can potentially control the relative importance of winter oceanic nitrate supply to spring biomass production on the adjacent shelf. Whilst our study clearly identifies differing cross-shelf transport regimes between the north and south, the sparsity of nutrient measurements and reliance upon a monthly nitrate climatology placed limitations on our analysis. We are unable to account for factors such as the interannual variability in the nitrate concentrations within the ocean nitrate pool or the strength of vertical nitrate gradients. These factors could be driven by changes in the source and pathways of subpolar and subtropical origin waters that are advected across the North Atlantic towards the shelf edge. Also, our timeseries of MLD for each sector relaxes to a climatological value where no direct observations of temperature were made, introducing unknown biases in some years. These limitations highlight the need for sustained biogeochemical and hydrographic sampling both on- and off-shelf, at a frequency of at least every month, to enable the full suite of physical and biogeochemical processes that determine variability in nitrate supply to the shelf to be better quantified and understood.

Data Availability Statement

All data used in this study are freely available online. The monthly subsurface temperature was obtained from the EN4 quality controlled ocean data (Good et al., 2013), https://www.metoffice.gov.uk/hadobs/en4/. The monthly climatologies of nitrate concentration, temperature and salinity were downloaded from the World Ocean Atlas 2018 (Boyer et al., 2018), https://www.ncei.noaa.gov/access/world-ocean-atlas-2018/. The monthly averaged surface stress data was obtained from the ERA5 global reanalysis (Hersbach et al., 2020): https://cds.climate.copernicus.eu/cdsapp#!/dataset/reanalysis-era5-single-levels-monthly-means?tab=overview. The monthly climatologies of

nitrate concentration on and off the shelf break were calculated from the North Sea Biogeochemical Climatology (Hinrichs et al., 2017), available at https://www.cen.uni-hamburg.de/en/icdc/data/ocean/nsbc.html.

Acknowledgments
The authors acknowledge funding from the NERC CLASS project (NE/R015953/1). This research has also received funding from the European Union's Horizon 2020 research and innovation programme under grant agreement No 818123 (iAtlantic). This output reflects only the author's view and the European Union cannot be held responsible for any use that may be made of the information contained therein. We acknowledge helpful comments provided by two anonymous reviewers which contribute to improving our paper.

References

Akpınar, A., Charria, G., Theetten, S., & Vandermeirsch, F. (2020). Cross-shelf exchanges in the northern Bay of Biscay. *Journal of Marine Systems*, *205*, 103314. https://doi.org/10.1016/j.jmarsys.2020.103314

Behrenfeld, M. J., Boss, E., Siegel, D. A., & Shea, D. M. (2005). Carbon-based ocean productivity and phytoplankton physiology from space. *Global Biogeochemical Cycles*, *19*(1), 605–620. https://doi.org/10.1029/2004gb002299

Boyer, T. P., Garcia, H. E., Locarnini, R. A., Zweng, M. M., Mishonov, A. V., Reagan, J. R., et al. (2018). World Ocean Atlas 2018 [Dataset]. NCEI. Retrieved from https://www.ncei.noaa.gov/archive/accession/NCEI-WOA18

Chaichana, S., Jickells, T., & Johnson, M. (2019). Interannual variability in the summer dissolved organic matter inventory of the North Sea: Implications for the continental shelf pump. *Biogeosciences*, *16*(5), 1073–1096. https://doi.org/10.5194/bg-16-1073-2019

Clark, M., Marsh, R., & Harle, J. (2022). Weakening and warming of the European slope current since the late 1990s attributed to basin-scale density changes. *Ocean Science*, *18*(2), 549–564. https://doi.org/10.5194/os-18-549-2022

Field, C. B., Behrenfeld, M. J., Randerson, J. T., & Falkowski, P. (1998). Primary production of the biosphere: Integrating terrestrial and oceanic components. *Science*, *281*(5374), 237–240. https://doi.org/10.1126/science.281.5374.237

Good, S. A., Martin, M. J., & Rayner, N. A. (2013). En4: Quality controlled ocean temperature and salinity profiles and monthly objective analyses with uncertainty estimates. *Journal of Geophysical Research: Oceans*, *118*(12), 6704–6716. https://doi.org/10.1002/2013jc009067

Gröger, M., Maier-Reimer, E., Mikolajewicz, U., Moll, A., & Sein, D. (2013). NW European shelf under climate warming: Implications for open ocean–shelf exchange, primary production, and carbon absorption. *Biogeosciences*, *10*(6), 3767–3792. https://doi.org/10.5194/bg-10-3767-2013

Hahn-Woernle, L., Dijkstra, H., & Van der Woerd, H. (2014). Sensitivity of phytoplankton distributions to vertical mixing along a North Atlantic transect. *Ocean Science*, *10*(6), 993–1011. https://doi.org/10.5194/os-10-993-2014

Hartman, S., Hartman, M. C., Hydes, D. J., Jiang, Z.-P., Smythe-Wright, D., & González-Pola, C. (2014). Seasonal and inter-annual variability in nutrient supply in relation to mixing in the Bay of Biscay. *Deep Sea Research Part II: Topical Studies in Oceanography*, *106*, 68–75. https://doi.org/10.1016/j.dsr2.2013.09.032

Hartman, S., Larkin, K., Lampitt, R., Lankhorst, M., & Hydes, D. (2010). Seasonal and inter-annual biogeochemical variations in the Porcupine Abyssal Plain 2003–2005 associated with winter mixing and surface circulation. *Deep Sea Research Part II: Topical Studies in Oceanography*, *57*(15), 1303–1312. https://doi.org/10.1016/j.dsr2.2010.01.007

Heath, M. R., & Beare, D. J. (2008). New primary production in northwest European shelf seas, 1960–2003. *Marine Ecology Progress Series*, *363*, 183–203. https://doi.org/10.3354/meps07460

Hersbach, H., Bell, B., Berrisford, P., Hirahara, S., Horányi, A., Muñoz-Sabater, J., et al. (2020). The ERA5 global reanalysis [Dataset]. Quarterly Journal of the Royal Meteorological Society, *146*(730), 1999–2049. https://doi.org/10.1002/qj.3803

Hinrichs, I., Gouretski, V., Pätsch, J., Emeis, K.-C., & Stammer, D. (2017). North Sea Biogeochemical climatology (version 1.1) [Dataset]. WDC Climate. https://doi.org/10.1594/WDCC/NSBClim_v1.1

Holt, J., Butenschön, M., Wakelin, S., Artioli, Y., & Allen, J. (2012). Oceanic controls on the primary production of the northwest European continental shelf: Model experiments under recent past conditions and a potential future scenario. *Biogeosciences*, *9*(1), 97–117. https://doi.org/10.5194/bg-9-97-2012

Holt, J., Wakelin, S., & Huthnance, J. (2009). Down-welling circulation of the northwest European continental shelf: A driving mechanism for the continental shelf carbon pump. *Geophysical Research Letters*, *36*(14), L14602. https://doi.org/10.1029/2009gl038997

Humphreys, M. P., Achterberg, E. P., Hopkins, J. E., Chowdhury, M. Z., Griffiths, A. M., Hartman, S. E., et al. (2019). Mechanisms for a nutrient-conserving carbon pump in a seasonally stratified, temperate continental shelf sea. *Progress in Oceanography*, *177*, 101961. https://doi.org/10.1016/j.pocean.2018.05.001

Huthnance, J. M., Hopkins, J., Berx, B., Dale, A., Holt, J., Hosegood, P., et al. (2022). Ocean shelf exchange, NW European shelf seas: Measurements, estimates and comparisons. *Progress in Oceanography*, *202*, 102760. https://doi.org/10.1016/j.pocean.2022.102760

Hydes, D. J., Le Gall, A., Miller, A., Brockmann, U., Raabe, T., Holley, S., et al. (2001). Supply and demand of nutrients and dissolved organic matter at and across the NW European shelf break in relation to hydrography and biogeochemical activity. *Deep Sea Research Part II: Topical Studies in Oceanography*, *48*(14–15), 3023–3047. https://doi.org/10.1016/s0967-0645(01)00031-5

Johnson, C., Inall, M., & Häkkinen, S. (2013). Declining nutrient concentrations in the northeast Atlantic as a result of a weakening Subpolar Gyre. *Deep Sea Research Part I: Oceanographic Research Papers*, *82*, 95–107. https://doi.org/10.1016/j.dsr.2013.08.007

Jones, S., Cottier, F., Inall, M., & Griffiths, C. (2018). Decadal variability on the Northwest European continental shelf. *Progress in Oceanography*, *161*, 131–151. https://doi.org/10.1016/j.pocean.2018.01.012

Jones, S., Inall, M., Porter, M., Graham, J. A., & Cottier, F. (2020). Storm-driven across-shelf oceanic flows into coastal waters. *Ocean Science*, *16*(2), 389–403. https://doi.org/10.5194/os-16-389-2020

Kitidis, V., Shutler, J. D., Ashton, I., Warren, M., Brown, I., Findlay, H., et al. (2019). Winter weather controls net influx of atmospheric CO_2 on the north-west European shelf. *Scientific Reports*, *9*(1), 1–11. https://doi.org/10.1038/s41598-019-56363-5

Koul, V., Schrum, C., Düsterhus, A., & Baehr, J. (2019). Atlantic inflow to the North Sea modulated by the subpolar Gyre in a historical simulation with MPI-ESM. *Journal of Geophysical Research: Oceans*, *124*(3), 1807–1826. https://doi.org/10.1029/2018jc014738

Laruelle, G. G., Dürr, H. H., Slomp, C. P., & Borges, A. V. (2010). Evaluation of sinks and sources of CO_2 in the global coastal ocean using a spatially-explicit typology of estuaries and continental shelves. *Geophysical Research Letters*, *37*(15), L15607. https://doi.org/10.1029/2010gl043691

Liu, K.-K., Atkinson, L., Quiñones, R. A., & Talaue-McManus, L. (2010). Biogeochemistry of continental margins in a global context. In *Carbon and nutrient fluxes in continental margins* (pp. 3–24). Springer.

Martin, A. P., Lucas, M. I., Painter, S. C., Pidcock, R., Prandke, H., Prandke, H., & Stinchcombe, M. C. (2010). The supply of nutrients due to vertical turbulent mixing: A study at the porcupine Abyssal Plain study site in the northeast Atlantic. *Deep Sea Research Part II: Topical Studies in Oceanography*, *57*(15), 1293–1302. https://doi.org/10.1016/j.dsr2.2010.01.006

Mathis, M., Elizalde, A., & Mikolajewicz, U. (2019). The future regime of Atlantic nutrient supply to the northwest European Shelf. *Journal of Marine Systems*, *189*, 98–115. https://doi.org/10.1016/j.jmarsys.2018.10.002

Mathis, M., Elizalde, A., Mikolajewicz, U., & Pohlmann, T. (2015). Variability patterns of the general circulation and sea water temperature in the North Sea. *Progress in Oceanography*, *135*, 91–112. https://doi.org/10.1016/j.pocean.2015.04.009

Mathis, M., & Mikolajewicz, U. (2020). The impact of meltwater discharge from the Greenland ice sheet on the Atlantic nutrient supply to the northwest European shelf. *Ocean Science*, *16*(1), 167–193. https://doi.org/10.5194/os-16-167-2020

Omand, M. M., & Mahadevan, A. (2015). The shape of the oceanic nitracline. *Biogeosciences*, *12*(11), 3273–3287. https://doi.org/10.5194/bg-12-3273-2015

Oschlies, A. (2002). Nutrient supply to the surface waters of the North Atlantic: A model study. *Journal of Geophysical Research*, *107*(C5), 14–21. https://doi.org/10.1029/2000jc000275

Pätsch, J., Gouretski, V., Hinrichs, I., & Koul, V. (2020). Distinct mechanisms underlying interannual to decadal variability of observed salinity and nutrient concentration in the northern North Sea. *Journal of Geophysical Research: Oceans*, *125*(5), e2019JC015825. https://doi.org/10.1029/2019jc015825

Pauly, D., Christensen, V., Guénette, S., Pitcher, T. J., Sumaila, U. R., Walters, C. J., et al. (2002). Towards sustainability in world fisheries. *Nature*, *418*(6898), 689–695. https://doi.org/10.1038/nature01017

Pingree, R., Griffiths, D., & Mardell, G. (1984). The structure of the internal tide at the Celtic Sea shelf break. *Journal of the Marine Biological Association of the United Kingdom*, *64*(1), 99–113. https://doi.org/10.1017/s002531540005966x

Pingree, R., Mardell, G., & New, A. (1986). Propagation of internal tides from the upper slopes of the Bay of Biscay. *Nature*, *321*(6066), 154–158. https://doi.org/10.1038/321154a0

Pohlmann, T. (1996). Calculating the annual cycle of the vertical eddy viscosity in the north sea with a three-dimensional baroclinic shelf sea circulation model. *Continental Shelf Research*, *16*(2), 147–161. https://doi.org/10.1016/0278-4343(94)e0037-m

Porter, M., Inall, M., Green, J., Simpson, J., Dale, A., & Miller, P. (2016). Drifter observations in the summer time Bay of Biscay slope current. *Journal of Marine Systems*, *157*, 65–74. https://doi.org/10.1016/j.jmarsys.2016.01.002

Ricker, M., & Stanev, E. V. (2020). Circulation of the European northwest shelf: A Lagrangian perspective. *Ocean Science*, *16*(3), 637–655. https://doi.org/10.5194/os-16-637-2020

Rodrigo, F. S. (2021). Exploring combined influences of seasonal East Atlantic (EA) and North Atlantic Oscillation (NAO) on the temperature-precipitation relationship in the Iberian Peninsula. *Geosciences*, *11*(5), 211. https://doi.org/10.3390/geosciences11050211

Roobaert, A., Laruelle, G. G., Landschützer, P., Gruber, N., Chou, L., & Regnier, P. (2019). The spatiotemporal dynamics of the sources and sinks of CO_2 in the global coastal ocean. *Global Biogeochemical Cycles*, *33*(12), 1693–1714. https://doi.org/10.1029/2019gb006239

Ruiz-Castillo, E., Sharples, J., Hopkins, J., & Woodward, M. (2019). Seasonality in the cross-shelf physical structure of a temperate shelf sea and the implications for nitrate supply. *Progress in Oceanography*, *177*, 101985. https://doi.org/10.1016/j.pocean.2018.07.006

Sharples, J., Mayor, D. J., Poulton, A. J., Rees, A. P., & Robinson, C. (2019). *Shelf Sea biogeochemistry: Nutrient and carbon cycling in a temperate shelf sea water column* (Vol. 177). Elsevier.

Sheehan, P. M., Berx, B., Gallego, A., Hall, R. A., Heywood, K. J., & Hughes, S. L. (2017). Thermohaline forcing and interannual variability of northwestern inflows into the northern North Sea. *Continental Shelf Research*, *138*, 120–131. https://doi.org/10.1016/j.csr.2017.01.016

Smith, S., & Banke, E. (1975). Variation of the sea surface drag coefficient with wind speed. *Quarterly Journal of the Royal Meteorological Society*, *101*(429), 665–673. https://doi.org/10.1002/qj.49710142920

Thomas, H., Bozec, Y., Elkalay, K., & De Baar, H. J. (2004). Enhanced open ocean storage of CO_2 from shelf sea pumping. *Science*, *304*(5673), 1005–1008. https://doi.org/10.1126/science.1095491

Tsunogai, S., Watanabe, S., & Sato, T. (1999). Is there a "continental shelf pump" for the absorption of atmospheric CO_2? *Tellus B: Chemical and Physical Meteorology*, *51*(3), 701–712. https://doi.org/10.1034/j.1600-0889.1999.t01-2-00010.x

Woollings, T., & Blackburn, M. (2012). The North Atlantic jet stream under climate change and its relation to the NAO and EA patterns. *Journal of Climate*, *25*(3), 886–902. https://doi.org/10.1175/jcli-d-11-00087.1